Materials Research Proceedings 41 (2024) 1752-1760 https://doi.org/10.21741/9781644903131-194

Inverse identification of the heterogeneous strain hardening of the friction stir welded aluminum sheets using virtual fields method

KIM Chanyang[1,a *], LEE Jinwoo[2,b *], KIM Daeyong[3,c] and LEE Myoung-Gyu [4,d *]

[1]Korea Institute of Materials Science, 797, Changwon-daero, Seongsan-gu, Changwon-si, Gyeongsangnam-do 51508, Republic of Korea

[2]School of Mechanical Engineering, University of Ulsan, 93, Daehak-ro, Nam-gu, Ulsan 44610, Republic of Korea

[3]Department of Intelligent Mobility, Chonnam National University, 77 Yongbong-ro, Buk-gu, Gwangju 61186, Republic of Korea

[a]c.kim@snu.ac.kr, [b]jinwoolee@ulsan.ac.kr, [c]daeyong.kim@jnu.ac.kr, [d]myounglee@snu.ac.kr

Keywords: FSW, VFM, Inverse Method, Local Plastic Strain Hardening, Aluminum Alloys

Abstract. In this paper, inverse identification of the local heterogeneous strain hardening in friction stir welded aluminum alloy sheets using a single tensile test is presented. During friction stir welding, the mechanical properties of the jointed aluminum sheets are altered from their original states. The finite element-based virtual fields method (FE-VFM) was applied to measure this change in the mechanical properties during the joining. Special numerical schemes were adopted in the FE-VFM for the accurate and numerically efficient identification of the local properties, including a two-step VFM calculation procedure, a sub-zone division approach in the weld-affected zone, quadratic interpolation of the constitutive parameters, and a special type of virtual fields based on the Gauss distribution function. The newly developed method was applied to measure strain-hardening distributions of the friction stir welded AA6061-T6 sheets. The measured distributions of the local strain hardening well captured decreased strength in the narrow thermo-mechanically affected zone (TMAZ). Finally, inversely measured mechanical properties were validated based on finite element analysis.

Introduction

Friction stir welding (FSW) is a solid-state joining process of metals, invented by The Welding Institute (TSW) [1]. In this process, the FSW tool rotates in between two workpieces, and frictional heat is generated. Materials soften owing to the uprising temperature in solid states, and mechanically stired and joined. The joining of the materials is proceeded by the translation forward of the FSW tools with the rotations. Microstructures of the materials in the weld-affected zone (WAZ) change majorly due to the heat, and mechanical properties can also be altered from the base material properties, subsequently. Particularly for the aluminum alloys, mechanical properties in the WAZ may decrease since the distribution distance and size of the precipitation deviate from the optimal state that was achieved in the previous heat treatment process in the base sheet material manufacturing [2]. This decrease in strength in the FSW of the aluminum alloys is critical for the evaluation or prediction of the performance in the post-FSW forming process.

As per the mechanical properties in the WAZ, assessing plastic strain hardening locally varied in the WAS is important. Distributions of the (micro) hardness are widely adopted conventionally, to evaluate strength changes in the WAZ [3,4]. However, Hardness distributions only can give relative changes in strength compared to the original base material properties, not the absolute information like the full stress-strain curves. A reliable method that can directly measure local full stress-strain curves in the WAZ is conducting miniature or micro tensile tests [5,6], but it demands multiple tests and relatively complex specimen fabrications. To overcome this issue, inverse

identification approaches were applied for the evaluation of the local plastic hardening in the WAZ such as the uniform or non-uniform stress method (USM or nUSM) [7,8], finite element model updating (FEMU) [9], and the virtual fields method (VFM) [8,10,11,12,13]. These methods all utilize strain distributions in the test specimen measured by the full-field measurement technique, such as the digital image correlation (DIC).

To measure the spatially changing mechanical properties within the WAZ using VFM, it is necessary to define the spatial dependency at the level of the constitutive model or its parameters. In the previous research, two major approaches were used. The straightforward approach is dividing an analyzed area of interest (AOI) in the VFM into sub-zones with equal step lengths [10,11,12,13]. Then, constitutive parameters in each sub-zone are assumed to be constant. This approach may be easy, but there are two disadvantages. In terms of resolution in the inverse measurement result, a small step length is favorable. However, the error included in the results is also increased for the smaller step lengths that are coming from inevitable noise in the non-contact type full-field measurements. In other words, accuracy and resolution can be in a trade-off relation depending on the step length size. Also, all the sub-zone material properties in the entire AOI were identified in the previous works. However, most of the welded materials remain as base material, and only the materials in the limited WAZ change from their original properties. Hence, it is numerically inefficient to measure already known, or easily obtainable base material properties. The other approach was predefining sub-zones considering the materials' microstructure [8]. The WAZ in the FSWed metals can be divided into fusion zone (FZ), thermo-mechanically affected zone (TMAZ), and heat affected zone (HAZ) [1]. These zones have distinctive characteristics on the microstructure. Hence, predefining a sub-zone is possible by the characterization of welded metals' microstructure, or through the hardness distribution measurements, indirectly. This approach enables to defining of good sub-zone divisions that coincide with the material characteristics, but it requires the preliminary procedure before applying the VFM. Nevertheless, both approaches assume the constant constitutive parameters within each sub-zone, and discontinuous material properties were assumed as a result.

In this study, the VFM was applied in measuring local strain hardening distributions in the WAZ of the friction stir welded (FSWed) AA6061-T6 sheets with a single tensile test [14]. In particular, finite element-based VFM (FE-VFM), which is an advanced formulation of the conventional VFM by adapting finite element schemes, was used [15]. Advanced numerical schemes in the VFM introduced in this research are as follows. A two-step identification procedure was applied, in which, the WAZ boundaries that material properties were varied from the base materials were inversely identified. Then, variations of the local strain hardening behavior (or the full stress-strain curves) were measured within the pre-identified WAZ, for the sake of efficient inverse measurements process. The VFM analyzed AOI was divided into several sub-zones, and the parameter distributions of the strain hardening laws were defined as a piecewise quadratic interpolation function. By doing so, continuous and quadratically varied distributions of the mechanical properties can be obtained within each sub-zone, rather than discontinuous and single constant values. Lastly, a special type of virtual field based on the Gaussian normal distribution function was introduced, which is for spatially employing strain (or stress) data at a certain range and uniquely obtaining mechanical property variations within each sub-zone. Finally, an in-depth discussion of the obtained distributions of the local strain hardening behavior and validation of the inverse measurements are presented in the result and discussion section.

Finite element-based virtual fields method (FE-VFM)

The VFM is an inverse technique to measure the mechanical properties of materials from full-field deformation measurements, theoretically relying on the principle of virtual works in Eq. (1).

Materials Research Proceedings 41 (2024) 1752-1760 https://doi.org/10.21741/9781644903131-194

$$\int_{\Omega} \boldsymbol{\sigma}(\boldsymbol{k}, \boldsymbol{\varepsilon}) \cdot \frac{\partial \delta \boldsymbol{u}}{\partial \boldsymbol{x}} dV = \int_{\partial \Omega_F} \boldsymbol{f}^{\mathbf{S}} \cdot \delta \boldsymbol{u} dS \quad (1)$$

In Eq. (1), the left and right terms are called internal and external virtual works. The virtual displacement fields $\delta \boldsymbol{u}$ and its derivatives $\frac{\partial \delta \boldsymbol{u}}{\partial \boldsymbol{x}}$ can be set by the VFM user, and actual strain fields and external forces $\boldsymbol{\varepsilon}$ and $\boldsymbol{f}^{\mathbf{S}}$ are measurable in the mechanical tests. Then, the only unknown in Eq. (1) is $\boldsymbol{k}$, which denotes the material parameters in constitutive law $\boldsymbol{\sigma}(\boldsymbol{k}, \boldsymbol{\varepsilon})$. In other words, unknown constitutive parameters can be obtained inversely by solving the principle of virtual work. For the linear elastic materials, Eq. (1) can be directly solved by constructing a system of linear equations using several independent virtual fields with the same number of unknown material constants [16]. However, for the elastic-plastic materials, Eq. (1) cannot be directly solved due to the nature of non-linear problems. Hence, non-linear minimization of the residuals between internal and external virtual works is performed to obtain the constitutive parameters [15].

The FE-VFM is an advanced formulation of conventional VFM borrowing the two major numerical approaches from the finite element method (FEM). The first important concept is mapping the displacements on the high-order finite element meshes rather than directly utilizing full-field measurements. The mapping procedure is as follows. First, the real initial coordinates of a target specimen are transformed on the natural coordinates which have regularized space in the -1 to 1 range, using the interpolation function depending on global initial coordinate values,

$$\mathbf{r} = \mathbf{M}(\mathbf{X_0})\mathbf{r^N} \quad (2)$$

where $\mathbf{r}$ and $\mathbf{X_0}$ denote natural and initial global coordinates, $\mathbf{M(X_0)}$ denotes high-order interpolation function, and uppercase $\mathbf{N}$ denotes nodal values. Then, displacements in each finite element can be described using the interpolation functions depending on the natural coordinate values,

$$\mathbf{u} = \mathbf{N}(\boldsymbol{r})\mathbf{u^N}. \quad (3)$$

In Eq. (3), nodal displacements in each time step are unknown initially, and these can be obtained using the Eqs. (2) and (3) and full displacement fields by the linear least square optimization.

Now then, all the upcoming numerical calculations can proceed just with the mapped displacements. Moreover, integration of the internal virtual work using the Gauss quadrature is possible, owing to the coordinate transformation from initial global to natural (or element) coordinates, and this is the second major scheme borrowing from the FEM. In summary, FE-VFM can achieve a numerically accurate and efficient process, owing to the high-order finite element interpolation and high-order Gauss quadrature.

Advanced numerical schemes in FE-VFM

Fig. 1(a) illustrates a tensile specimen for applying the FE-VFM in this work. In the specimen, the weld line was positioned at the center, and the specimen length direction was perpendicular to the weld line. Fig. 1(b) is a 3rd other finite element meshes used in the FE-VFM. The blue-marked region in Fig. 1(a) was analyzed by the FE-VFM. The length (or height) of an element was 3 mm, and each low of elements was assumed as a single sub-zone. Note that numerical analysis in the FE-VFM was applied on the unit of a sub-zone independently, not the whole AOI simultaneously. The total number of constitutive parameters in the whole WAZ is a lot larger compared to the homogeneous material case, to describe spatial distributions. Hence, constitutive parameters might not be uniquely optimized if all the constitutive parameters for all the sub-zones are identified together.

Fig. 1(c) schematically illustrates the two-step identification process introduced in this work. Prior to the FE-VFM analysis, uniaxial tensile tests for the base sheet metals are conducted, and the mechanical properties of the base materials are obtained. Then, virtual work residuals are calculated using the base material's constitutive parameters in each sub-zone, in STEP1. If materials are affected during the FSW, then residuals will be larger compared to those in not affected area, and boundaries of the WAZ can be easily identified. In STEP2, distributions of the hardening law parameters are optimized by minimizing virtual work residuals, for each sub-domain independently. The distributions of constitutive parameters within each sub-zone are quadratically interpolated,

$$\overline{k} = \boldsymbol{Q}(Y)\overline{\boldsymbol{k}}^{\boldsymbol{N}} = [1 \quad Y \quad Y^2]\begin{bmatrix} 0 & 1 & 0 \\ \frac{1}{3} & 0 & \frac{1}{3} \\ \frac{2}{9} & \frac{-4}{9} & \frac{2}{9} \end{bmatrix}\begin{bmatrix} \overline{k}^1 \\ \overline{k}^2 \\ \overline{k}^3 \end{bmatrix} \tag{4}$$

where $\overline{k}$ is constitutive parameters normalized by its based material values, and Y is coordinate value in the length direction of the specimen which has zero values at the center of each sub-zone, and the nodal position in parameter interpolation is located Y=1.5, 0, and -1.5 for node number (uppercase in Eq. (4)) 1,2, and 3.

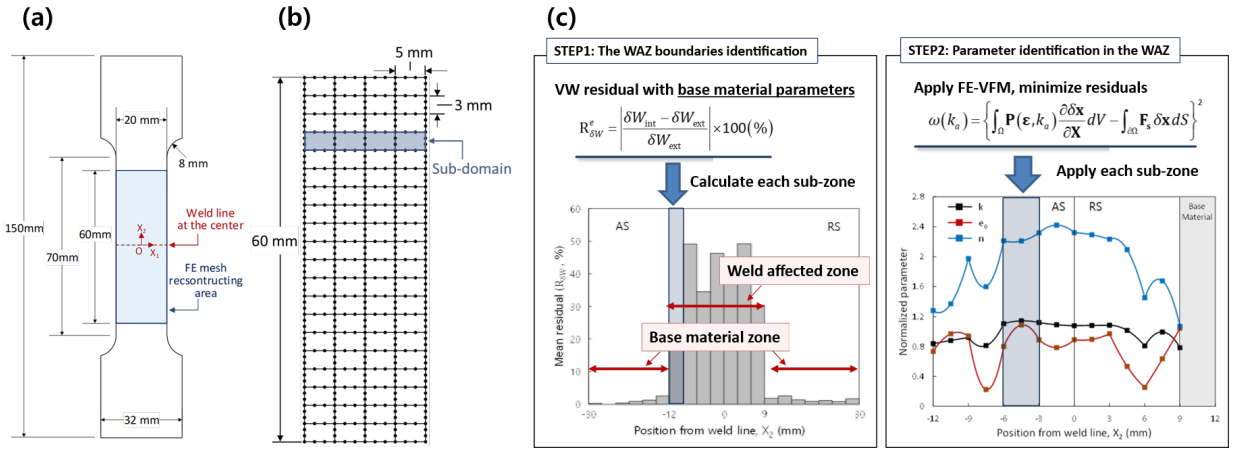

Fig. 1. (a) Specimen geometries for applying the FE-VFM. (b) Cubic quadrilateral high-order finite element (FE) meshes used in the FE-VFM. (c) Two-step identification procedure.

The isotropic constitutive model was used in this research, the generalized Hooke's law and the von Mises yield criteria were used. The Swift hardening law was used,

$$\bar{\sigma} = K(\bar{\varepsilon} + e_0)^n. \tag{5}$$

Material constants of the base material AA6061-T6 sheets are listed in Table 1. In inverse measurements using the FE-VFM, only Swift hardening law parameters were optimized in STEP2, considering that the elastic constants are not significantly changed owing to the thermal histories. Also, note that normalized-nodal constitutive parameters of the Swift law were identified in STEP2 (denoted $\overline{k}$ in Eq. (4)), and real parameter distributions can be described by multiplying the values of the base materials in Table 1 and Eq. (5).

Table 1. Elastic constants and the Swift law parameters of the AA6061-T6 sheets.

Elastic constants		Swift law parameters		
E [GPa]	ν	K [MPa]	e_0	n
70	0.33	508.1	0.03602	0.1577

Meanwhile, quadratic interpolation of the constitutive parameters makes it hard to uniquely identify when conventional types of virtual fields are employed. It is because of that the three nodal-normalized constitutive material parameters are interconnected quadratically in each sub-zone, and a wrong combination of the nodal values can give a false zero residuals. A special type of virtual field is introduced to avoid this issue, based on the Gaussian normal distribution function. The virtual position field is defined as,

$$\delta x_1 = \begin{cases} X_1(Y^2 - 2.25)(|Y| \le 1.5) \\ 0(|Y| > 1.5) \end{cases}, \delta x_2 = \begin{cases} \Phi_{i=1,2,3}(Y)(|Y| \le 1.5) \\ 0(|Y| > 1.5) \end{cases} \tag{6}$$

where $\Phi_{i=1,2,3}$ is the cumulative distribution function,

$$\Phi_{i=1,2,3}(Y) = \frac{1}{2}\left\{1 + \mathrm{erf}\left(\frac{Y-\mu_i}{\sigma_N\sqrt{2}}\right)\right\}. \tag{7}$$

Then, the derivatives of the virtual position, or the virtual deformation gradient is given as

$$\delta \boldsymbol{F} = \frac{\partial \delta \boldsymbol{x}}{\partial \boldsymbol{X}} = \begin{pmatrix} Y^2 - 2.25 & 2X_1Y \\ 0 & \varphi_{i=1,2,3}(Y) \end{pmatrix} \tag{8}$$

where $\varphi_{i=1,2,3}$ is the Gaussian normal distribution function,

$$\varphi_{i=1,2,3}(Y) = \frac{1}{\sigma_N\sqrt{2\pi}} exp\left\{-\frac{1}{2}\left(\frac{Y-\mu_i}{\sigma_N}\right)^2\right\}. \tag{9}$$

The Gaussian distribution can act as an amplifier of the strain (or stress) data within a target range in the sub-zones, when different σ_N and μ_i are adopted. In this work, three independent virtual fields with values of $\sigma_N = 0.5$ and μ_i= 1, 0, −1 for i=1,2,3 were used. Fig. 2 schematically illustrates the role of the Gaussian distribution type virtual fields. The σ_N in Gaussian distribution determines the width of a larger value area, 2σ. Considering that the length of the sub-zone is 3 mm, $\sigma_N = 0.5$ is used. Also, μ_i determines the peak location in the Gaussian distribution, and three different μ_i= 1, 0, −1 are applied. Consequently, three independent virtual fields amplify the mechanical data of the top, middle, and bottom regions, selectively. Owing to these three Gaussian distribution-type virtual fields, three nodal-normalized constitutive parameters can be uniquely optimized despite that these parameters are interconnected with quadratic interpolation functions.

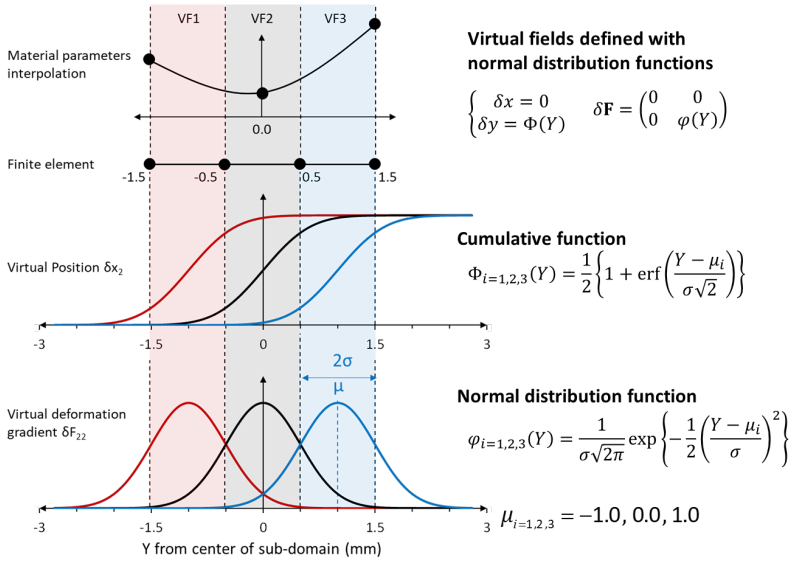

Fig. 2. The Gaussian normal distribution type virtual fields for amplifying data in different regions in the sub-zone.

Materials and experiments

The friction stir welded AA6061-T6 sheets were investigated. The thickness of the base material sheets was 3 mm. Rectangular workpieces of 300 mm x 150 mm were joined into 300 mm size foursquare sheets. The FSW conditions were as follows. The pin of the FSW tool was truncated cone shape, with a smaller bottom diameter and larger top diameter of 4 and 6 mm. The diameter of the FSW tool shoulder was 12.72 mm. The tool travel speed was 500 mm/min. The FSW was conducted with two conditions, with tool rotation speeds of 1200 and 1600 RPM.

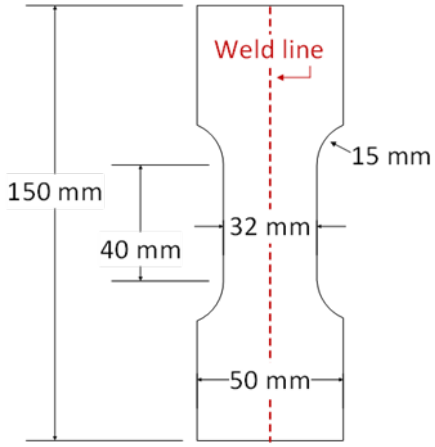

Fig. 3. Schematic illustration of the validation tensile test specimens.

The tensile specimens for applying the FE-VFM were made by wire electric discharge machining (W-EDM) following the geometries in Fig. 1(a). The FSW process remains a trace of the tool path like a plumbing groove. So, the surface of the tensile specimen was trimmed by the W-EDM, and the thickness of the specimen was reduced to 2.3 mm. For the validation of the measured local strain hardening distributions, a different configuration of tensile tests Was conducted, which loaded along the weld line direction, as shown in Fig. 3. These test results were compared with the FEM predictions conducted with the inverse measurements.

All the tensile tests were conducted with the same condition. Instron 8801 100 kN UTM was used, and the test speed was 1 mm/min, which is within quasi-static conditions. Deformations were measured by the commercial DIC packages, the VIC-3D. In the validation tensile tests, displacements were measured by the virtual extensometer with a gauge length of 40 mm in DIC post-analysis, and the force-displacement curves measured by this were compared with the validation FEM predictions.

Result and discussion

Fig. 4(a) shows the virtual work residuals (VWR) for each sub-zone in STEP1, which were calculated using the base material properties in Table 1. The VWR shows considerably larger values from the -12 to 9 mm range for the 1200 RPM case, and the -12 to 12 mm range for the

1600 mm case. These regions are the WAZ, and the outside regions are the base materials unaffected by the FSW process. This result indicates that the WAZ is smaller for the 1200 RPM case compared to the 1600 RPM case, on the retreating side (RS). The RS is a side where the direction of rotation and tool translation direction are opposite, and heat generated during the FSW is smaller compared to the advancing side (AS). For the 1200 RPM, less frictional heat would generated compared to the 1600 RPM, and the smaller WAZ can be formed.

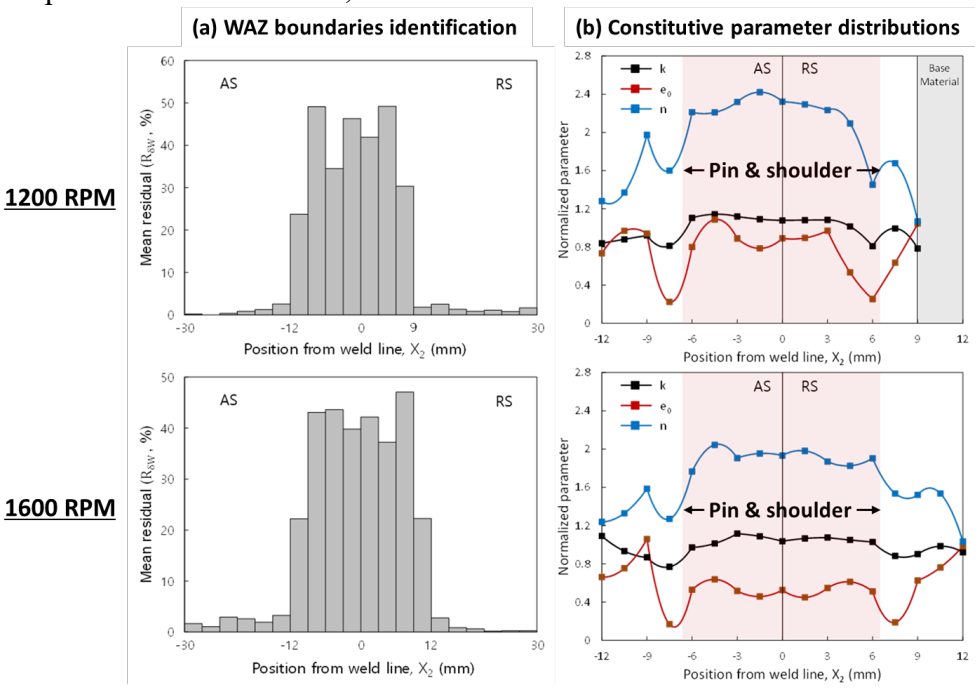

Fig. 4. Inverse identifiaction results. (a) Virtual work residuals for each sub-zone in the WAZ boundaries identification (in STEP1). (b) Distributions of the normal-normalized constitutive parameters in the Swift laws (in STEP2).

Fig. 4(b) shows distributions of the constitutive parameters in the Swift laws. Note that solid lines are the quadratic interpolations of the normalized values by base material values, and the square dotes denote nodal-normalized values which are the 1st direct inverse measurements in this work. It can be seen that the parameter n values within the -6 to 6 mm range exhibit almost twice larger than the base material value for both 1200 and 1600 RPM cases. The Swift law parameter n is highly related to the uniform elongation by the Considère condition. Also, this region is exactly matched with the diameter of the FSW tool shoulder. Hence, this result indicates that welded materials were softened by the FSW process. Also, rapid drops of the n values are found just near and outside of this range, which corresponds to the thermo-mechanically affected zone (TMAZ). A lower n value indicates a shorter uniform elongation in the tensile tests, and the n value was only around 40% compared to the base material properties. The TMAZ is typically considered to be a weak location in the FSWed sheets, hence, the result of sudden valley-shape distributions of n value in this area can be interpreted that the lower uniform elongation was measured in these relatively narrow TMAZ regions.

Fig. 5 shows the force-displacement curves in the validation tensile tests loaded in weld line directions. The FEM analyses were conducted by using the distributions of the local strain hardening in Fig. 4(a). It can be noticed that the experimental values (empty circle dots) and FEM predictions (solid lines) show very good matches. This confirms that the suggested FE-VFM method can measure local strain hardening distributions of the welded sheets with good accuracy.

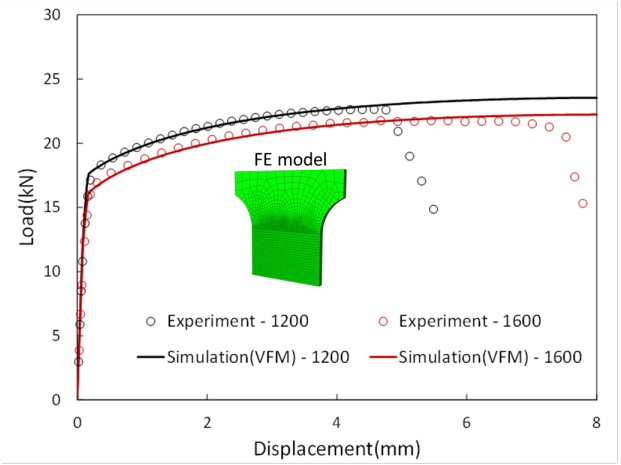

Fig. 5. Tensile tests and FEM analyses for the validation of the inverse measurements.

Summary

Inverse identification of the local strain hardening distributions for the FSWed AA6061-T6 sheets was conducted by the FE-VFM. In the FE-VFM, new numerical schemes were introduced, including the two-step identification procedure, the sub-zone independent identification with quadratic interpolation of the constitutive parameters, and the new Guass distribution function type virtual fields. Measured distributions of local strain hardening well capture a material softening due to the FSW process, and the weaker material properties in the TMAZ. Also, experimental force-displacement curves and the FEM predictions using the inverse measurements showed good matches in the validation tensile tests, which confirms the capability of the proposed inverse identification method.

Acknowledgment

This work was supported by the Fundamental Research Program of the Korea Institute of Materials Science (KIMS, PNK9800) and the National Research Council of Science and Technology (NST) grant by the Korea government (MSIT) (CRC23011-210).

References

[1] X. He, F. Gu, A. Ball, A review of numerical analysis of friction stir welding, Prog. Mat. Sci. 65 (2014) 1-66. https://doi.org/10.1016/j.pmatsci.2014.03.003

[2] D. Myung, W. Noh, J.-H. Kim, J. Kong, S.-T. Hong, M.-G. Lee, Probing the Mechanism of Friction Stir Welding with ALE Based Finite Element Simulations and Its Application to Strength Prediction of Welded Aluminum, Metals Mat. Int. 27 (2021) 650–666. https://doi.org/10.1007/s12540-020-00901-8

[3] G. Güleryüz, Relationship between FSW parameters and hardness of the ferritic steel joints: Modeling and optimization, Vacuum 178 (2020) 109449. https://doi.org/10.1016/j.vacuum.2020.109449

[4] J.H. Kim, F. Barlat, C. Kim, K. Chung, Themo-mechanical and microstructural modeling of friction stir welding of 6111-T4 aluminum alloys, Metals Mat. Int. 15 (2009) 125-132. https://doi.org/10.1007/s12540-009-0125-5

[5] D. Rao, J. Heerens, G. Alves Pinheiro, J.F. dos Santos, N. Huber, On characterisation of local stress-strain properties in friction stir welded aluminium AA5083 sheets using micro-tensile specimen testing and instrumented indentation technique, Mat. Sci. Eng. A 527 (2010) 5018-5025. https://doi.org/10.1016/j.msea.2010.04.047

[6] D. Bernard, D.G. Hattingh, W.E. Goosen, M.N. James, High Speed Friction Stir Welding of 5182-H111 Alloy: Temperature and Microstructural Insights into Deformation Mechanisms, Metals Mat. Int. 27 (2021) 2821-2836. https://doi.org/10.1007/s12540-020-00622-y

[7] G. Cao, M. Ren, Y. Zhang, W. Peng, T. Li, A partitioning method for friction stir welded joint of AA2219 based on tensile test, Metals 10 (2020) 65. https://doi.org/10.3390/met10010065

[8] M.A. Sutton, J.H. Yan, S. Avril, F. Pierron, S.M. Adeeb, Identification of heterogeneous constitutive parameters in a welded specimen: Uniform stress and virtual fields methods for material property estimation, Exp. Mech. 48 (2008) 451–464. https://doi.org/10.1007/s11340-008-9132-6

[9] F. Tucci, A. Andrade-Campos, S. Thuillier, P. Carlone, Calibration of the Elasto-Plastic Properties of Friction Stir Welded Blanks in Aluminum Alloy AA6082, Key Eng. Mater. 926 (2022) 2183–2192. https://doi.org/10.4028/p-3a8e45

[10] G. Le Louëdec, F. Pierron, M.A. Sutton, A.P. Reynolds, Identification of the Local Elasto-Plastic Behavior of FSW Welds Using the Virtual Fields Method, Exp. Mech. 53 (2013) 849–859. https://doi.org/10.1007/s11340-012-9679-0

[11] G. Le Louëdec, F, Pierron, M.A. Sutton, C. Siviour, A.P. Reynolds, Identification of the Dynamic Properties of Al 5456 FSW Welds Using the Virtual Fields Method, J. Dynamic Behavior Mater. 1 (2015) 176–190. https://doi.org/10.1007/s40870-015-0014-6

[12] C. Kim, J.H. Kim, M.-G. Lee, Identification of Inhomogeneous Plastic Constitutive Models of Friction Stir Welded Aluminum Alloy Sheets Using Virtual Fields Method, Conf. Proc. Soci. Exp. Mech. (2020) 157–161. https://doi.org/10.1007/978-3-030-30098-2_24

[13] H. Jiang, Z. Lei, R. Bai, W. Wu, et al., Identifying elasto-plastic damage coupling model of laser-welded aluminum alloy by virtual field method and digital image correlation, Opt. Laser Tech. 129 (2020) 106268. https://doi.org/10.1016/j.optlastec.2020.106268

[14] C. Kim, D. Myung, D. Kim, M.-G. Lee, Inhomogeneous flow stresses in FSW jointed aluminum alloy sheets inversely identified by FE-VFM, Int. J Mech. Sci. 245 (2023) 108097. https://doi.org/10.1016/j.ijmecsci.2022.108097

[15] C. Kim, M.-G. Lee, Finite element-based virtual fields method with pseudo-real deformation fields for identifying constitutive parameters, Int. J of Sol. Struct. 233 (2021) 111204. https://doi.org/10.1016/j.ijsolstr.2021.111204

[16] C. Kim, J.H. Kim, M.-G. Lee, A virtual fields method for identifying anisotropic elastic constants of fiber reinforced composites using a single tension test: Theory and validation, Composites Part B: Eng. 200 (2020) 108338. https://doi.org/10.1016/j.compositesb.2020.108338